Implementing quantum information processing with atoms, ions and photons *

P. Zoller¹, J. I. Cirac², Luming Duan³ and J. J. García-Ripoll²

¹Institute for Theoretical Physics, University of Innsbruck,
and Institute of the Austrian Academy of Sciences for Quantum Optics and Quantum Information, A-6020 Innsbruck, Austria

² Max-Planck-Institut für Quantenoptik, Hans-Kopfermann-Str. 1, Garching, D-85748, Germany and

³ Department of Physics and FOCUS center, University of Michigan, Ann Arbor, MI 48109

(Dated: 2003 08)

I. INTRODUCTION

Quantum optical systems are one of the very few examples of quantum systems, where complete control on the single quantum level can be realized in the laboratory, while at the same time avoiding unwanted interactions with the environment causing decoherence. These achievements are illustrated by storage and laser cooling of single trapped ions and atoms, and the manipulation of single photons in Cavity QED, opening the field of engineering interesting and useful quantum states. In the mean time the frontier has moved towards building larger composite systems of a few atoms and photons, while still allowing complete quantum control of the individual particles. The new physics to be studied in these systems is based on entangled states, both from a fundamental point of testing quantum mechanics for larger and larger systems, but also in the light of possible new applications like quantum information processing or precision measurements [1, 2].

Guided by theoretical proposals as reviewed in [3], we have seen extraordinary progress in experimental AMO physics during the last few years in implementing quantum information processing. Highlights are the recent accomplishments with ion traps[4], cold atoms in optical lattices [5], cavity QED (CQED) [6] and atomic ensembles [7]. Below we summarize some of the theoretical aspects of implementing quantum information processing with quantum optical systems. In particular, in Sec. II we discuss quantum computing with trapped ions. Sec. III demonstrates cold coherent collisions as a mean to entangle atoms in an optical lattice. Finally, Sec. IV reviews atomic ensembles.

II. TRAPPED IONS

Trapped ions is one of the most promising systems to implement quantum computation [3, 8, 9]. In this section we describe the theory of quantum information processing with a system of trapped ions. On the experimental side remarkable progress has been reported during the last two years in realizing some of the these ideas in the

laboratory[10, 11, 12], as explained in the lecture notes by R. Blatt and D. Wineland.

Ion trap quantum computing, as first proposed in [8], stores qubits in longlived internal states of single trapped ion. Single qubit gates are performed by coupling the qubit states to laser light for an appropriate period of time. In general, this requires that single ions can be addressed by laser light. Two qubit gates can be achieved by entangling ions via collective phonon modes. Depending on the specific protocol this requires the initialization of the phonon bus in a pure initial state, e.g. laser cooling to the motional ground state in ion traps. However, recently specific protocols for "hot gates" have been developed which loosen these requirements (see [3, 13] and references cited). The unitary operations, which can be decomposed in a series of single and two-qubit operations on the qubits, can either be performed dynamically, i.e. based on the time evolution generated by a specific Hamiltonian, or *geometrically* as in holonomic quantum computing [14]. Finally, read out of the atomic qubit is accomplished using the method of quantum jumps [15].

An essential feature of ion trap quantum computers is the scalability to a large number of qubits. This is achieved by moving ions from a storage area, either to address the ions individually to perform the single qubit rotation, or by bringing pairs of ions together to perform a two-qubit gate. Moving ions does not affect the qubit stored in the internal electronic or hyperfine states, and heating of the ion motion can cooled in a nondestructive way by sympathetic cooling [16, 17, 18].

In our discussion below we will start with a brief outline of manipulation of trapped ions by laser light. We then proceed to illustrate ion trap quantum computing with two specific examples. We will first discuss in some detail the basic physical ideas and requirements of the original ion trap proposal[8]. Our emphasis is on the two qubit gate, and in direct relation to experimental work described by R. Blatt and D. Wineland. As a second example, we discuss the most recent proposal for a fast and robust 2-qubit gates for scalable ion trap quantum computing, based on laser coherent control techniques [13]. This 2-qubit gate can be orders of magnitude faster than the time scale given by the trap period, thus overcoming previous speed limits of ion trap quantum computing, while at the same time relaxing the experimental constraints of individual laser addressing of the ions and cooling to low temperatures.

^{*}les Houches summer school proceedings, session 79, Ed. D. Estève, J.M. Raimond and J. Dalibard, Elsevier, Amsterdam (2004)

A. Modelling a single trapped ion

In this section we give a theoretical description of quantum state engineering in a system of trapped and laser cooled ions. The development of the theory begins with the description of Hamiltonians, state preparation, laser cooling and state measurements for single ions, and then followed by a generalization to the case of many ions. This serves as the basis of our discussion of quantum computer models.

We describe a single trapped ion driven by laser light as a two-level atom $|g\rangle, |e\rangle$ moving in a 1D harmonic confining potential [3] with Hamiltonian ($\hbar=1$)

$$H = \nu a^{\dagger} a - \frac{1}{2} \Delta \sigma_z + \frac{1}{2} \Omega \{ \sigma_+ e^{i\eta(a+a^{\dagger})} + \text{h.c.} \}. \tag{1}$$

Here the first term is the harmonic oscillator Hamiltonian for the center-of-mass motion of the ion with trap frequency ν . We have denoted by a and a^{\dagger} the lowering and raising operators, respectively, which can be expressed in terms of the position and momentum operators as $\hat{x} = \sqrt{1/2M\nu}(a+a^{\dagger})$ and $\hat{p} = i\sqrt{M\nu/2}(a^{\dagger}-a)$ with M the ion mass. The second and third term in 1 describe the driven two-level system in a rotating frame using standard spin- $\frac{1}{2}$ notation, $\sigma_+ = (\sigma_-)^\dagger = |e\rangle\langle g|$ and $\sigma_z = |e\rangle\langle e| - |g\rangle\langle g|$. This internal atomic Hamiltonian is written in a frame rotating with the optical frequency. We denote by $\Delta = \omega_L - \omega_{eg}$ the detuning of the laser with ω_L the laser frequency and by ω_{eg} the atomic transition frequency, and Ω is the Rabi frequency for the transition $|q\rangle \rightarrow |e\rangle$. In writing 1 we have assumed that the atom is driven by a running laser wave with wave vector $k_L = 2\pi/\lambda_L$ along the oscillator axis. Transitions from $|g\rangle$ to $|e\rangle$ are associated with a momentum kick to the atom by absorption of a laser photon, as described by $\exp(ik_L\hat{x}) \equiv \exp(i\eta(a+a^{\dagger}))$, which couples the motion of the ion (phonons) to the internal laser driven dynamics.

In Eq. (1) we have defined a Lamb-Dicke parameter $\eta = 2\pi a_0/\lambda_L$ with $a_0 0 \sqrt{1/2M\nu}$ the ground state size of the oscillator and λ_L the laser wave length. In the Lamb-Dicke limit $\eta \ll 1$ we can expand the atom laser interaction: $H_{AL} = \frac{1}{2}\Omega\{\sigma_{-}[1+i\eta(a+a^{\dagger})+\mathcal{O}(\eta^{2})]+\text{h.c.}\}.$ The resulting Hamiltonian can be further simplified if the laser field is sufficiently weak so that only pairs of bare atom + trap levels are coupled resonantly. We denote by $|g\rangle|n\rangle$ and $|e\rangle|n\rangle$ the eigenstates of the bare Hamiltonian $H_0 = \nu a^{\dagger} a - \frac{1}{2} \Delta \sigma_z$, where the internal two-level system is in the ground (excited) state and n is the phonon excitation number of the harmonic oscillator. When tuning the laser to atomic resonance $\Delta = \omega_L - \omega_{eg} \approx 0$, i.e. $|\omega_L - \omega_{eg}| \ll \nu$, the transitions changing the harmonic oscillator quantum number n are off-resonance and can be neglected. In this case the Hamiltonian (1) can be approximated by

$$H_0 = \nu a^{\dagger} a - \frac{1}{2} \Delta \sigma_z + \frac{1}{2} \Omega(\sigma_+ + \text{h.c.}) \quad (\Delta \approx 0), \quad (2)$$

On the other hand, for laser frequencies close to the lower (red) motional sideband resonance $\Delta \approx -\nu$, i.e.

 $|\omega_L - (\omega_{eg} - \nu)| \ll \nu$, only transitions decreasing the quantum number n by one are important, and H can be approximated by a Hamiltonian of the Jaynes-Cummings type:

$$H_{\rm JC} = \nu a^{\dagger} a - \frac{1}{2} \Delta \sigma_z + \frac{1}{2} \Omega(i \eta \sigma_+ a + \text{h.c.}) \quad (\Delta \approx -\nu).$$
 (3)

Similarly, for tuning to the upper (blue) sideband $\Delta \approx +\nu$, i.e. $\omega_L - (\omega_{eg} + \nu)| \ll \nu$, only transitions increasing the quantum number n by one contribute, so that H can be approximated by the anti-Jaynes-Cummings Hamiltonian

$$H_{\rm AJC} = \nu a^{\dagger} a - \frac{1}{2} \Delta \sigma_z + \frac{1}{2} \Omega (i \eta \sigma_+ a^{\dagger} + \text{h.c.}) \quad (\Delta \approx +\nu).$$
 (4)

(see Fig. II A) For the above approximations to be valid we require that the effective Rabi frequencies to the non-resonant states have to be much smaller than the trap frequency, i.e. we must spectroscopically resolve the motional sidebands.

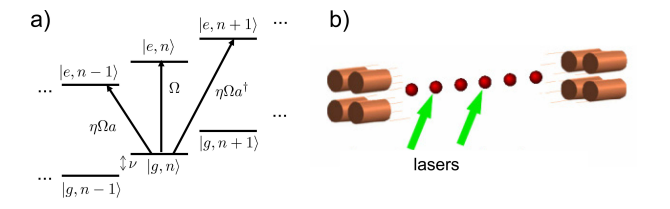


FIG. 1: a) Coupling to the atom + trap levels according to the Hamiltonians (2), (3 and (4, respectively, in lowest order Lamb-Dicke expansion. b) ion trap quantum computer 1995 (schematic)

The eigenstates of the Hamiltonians H_0 , $H_{\rm JC\pm}$ and $H_{\text{AJC}\pm}$ are the dressed states. These states are familiar from cavity QED, and are obtained by diagonalizing the $2x^2$ matrices of nearly degenerate states. Applying a laser pulse on resonance, $\Delta = 0$, will according to (2) induce Rabi flopping between the states $|g\rangle|n\rangle$ and $|e\rangle|n\rangle$, while a laser tuned for example to the lower motional sideband $\Delta = -\nu$ will lead to Rabi oscillations coupling $|g\rangle|n\rangle$ and $|e\rangle|n-1\rangle$. The above Hamiltonians are basic building blocks to engineer general quantum states of motion. As an example, a laser pulse applied on the carrier frequency ($\Delta = 0$) to a state $(\alpha | g \rangle + \beta | e \rangle) | 0 \rangle$ will induce a general Rabi rotation without affecting the phonon state, i.e. perform a single qubit rotation. On the other hand, a π -pulse with duration $T = \pi/\eta\Omega$ on the red sideband will swap an initial superposition of qubits to a corresponding superposition of phonon states, $(\alpha|g\rangle + \beta|e\rangle)|0\rangle \rightarrow |g\rangle(\alpha|0\rangle + \beta|1\rangle)$. These processes will be the building blocks for the quantum gate discussed below.

We note that the interaction time for the above processes must always be much longer than the trap period $1/\nu$. On the other hand, when we apply a short laser pulse to the ion much less than the trap period $1/\nu$, i.e. we do not spectroscopically resolve the sidebands, and we can ignore the trap motion during the time duration of the pulse. A π -pulse to the two level atom is thus accompanied by a momentum kick to the motional state $|g\rangle|\text{motion}\rangle \rightarrow |e\rangle e^{ik_L\hat{x}}|\text{motion}\rangle$, $|e\rangle|\text{motion}\rangle \rightarrow |e\rangle e^{-ik_L\hat{x}}|\text{motion}\rangle$. In particular, if we choose a coherent state $|\alpha\rangle_{\text{coh}}$ to represent the motion, we will shift the coherent states $|g\rangle|\alpha\rangle_{\text{coh}} \rightarrow |e\rangle|\alpha+i\eta\rangle_{\text{coh}}$, $|e\rangle|\alpha\rangle_{\text{coh}} \rightarrow |g\rangle|\alpha-i\eta\rangle_{\text{coh}}$. Furthermore, if we apply a short π -pulse in the direction $+k_L$ followed by a pulse from the opposite direction $-k_L$, we achieve a transformation

$$|g\rangle|\alpha\rangle_{\rm coh} \to |g\rangle|\alpha + 2i\eta\rangle_{\rm coh}$$

 $|e\rangle|\alpha\rangle_{\rm coh} \to |e\rangle|\alpha - 2i\eta\rangle_{\rm coh}$

This process will be the basic element of the high speed 2 qubit gate at the end of this section.

B. Ion trap quantum computer '95

We describe in some detail the 2-qubit gate in the original ion trap proposal, as illustrated in Fig. IIB. [8]. In the ion trap quantum computer'95 qubits are represented by the long-lived internal states of the ions, with $|g\rangle_i \equiv |0\rangle_i$ the ground state, and $|e_0\rangle_i \equiv |1\rangle_i$ a (metastable) excited state (j = 1, ..., N). In addition, we assume that there is a second metastable excited state $|e_1\rangle$ which plays below the role of an auxiliary state. In this system separate manipulation of each individual qubit is accomplished by addressing the ions with different laser beams and inducing a Rabi rotation. The heart of the proposal is the implementation of a two-qubit gate between two (or more) arbitrary ions in the trap by exciting the collective quantized motion of the ions with lasers, i.e. the collective phonon mode plays the role of a quantum data bus. For this we assume that the collective phonon modes have been cooled initially to the ground state.

Single qubit rotations can be performed tuning a laser on resonance with the internal transition $(\Delta_j = 0)$ with polarization q = 0, $|g\rangle_j \to |e_0\rangle_j$. In an interaction picture the corresponding Hamiltonian is

$$\hat{H}_{j} = \frac{1}{2} \Omega \left[|e_{0}\rangle_{j} \langle g|e^{-i\phi} + |g\rangle_{j} \langle e_{0}|e^{i\phi} \right]. \tag{5}$$

For an interaction time $t=k\pi/\Omega$ (i.e., using a $k\pi$ pulse), this process is described by the following unitary evolution operator

$$\hat{V}_{j}^{k}(\phi) = \exp\left[-ik\frac{\pi}{2}(|e_{0}\rangle_{j}\langle g|e^{-i\phi} + h.c.)\right], \quad (6)$$

so that we achieve a Rabi rotation

$$|g\rangle_j \longrightarrow |g\rangle_j \cos(k\pi/2) - |e_0\rangle_j ie^{i\phi} \sin(k\pi/2),$$

 $|e_0\rangle_j \longrightarrow |e_0\rangle_j \cos(k\pi/2) - |g\rangle_j ie^{-i\phi} \sin(k\pi/2).$

When we work with N ions, the ion chain supports N longitudinal modes, of which the center of mass mode, $\nu_1 = \nu$, is energetically separated from the rest, $\nu_k > = \sqrt{3}\nu$ (k > 1). If the laser addressing the j-th ion is tuned to the lower motional sideband of, for example, the center-of-mass mode, we have in the interaction picture the Hamiltonian

$$H_{j,q} = \frac{\eta}{\sqrt{N}} \frac{\Omega}{2} \left[|e_q\rangle_j \langle g|ae^{-i\phi} + |g\rangle_j \langle e_q|a^{\dagger}e^{i\phi} \right]. \tag{7}$$

Here a^\dagger and a are the creation and annihilation operator of the center-of-mass phonons, respectively, Ω is the Rabi frequency, ϕ the laser phase, and η is the Lamb-Dicke parameter. The subscript q=0,1 refers to the transition excited by the laser, which depends on the laser polarization.

If this laser beam is on for the time $t = k\pi/(\Omega\eta/\sqrt{N})$ (i.e., using a $k\pi$ pulse), the evolution of the system will be described by the unitary operator:

$$\hat{U}_{j}^{k,q}(\phi) = \exp\left[-ik\frac{\pi}{2}(|e_{q}\rangle_{j}\langle g|ae^{-i\phi} + h.c.)\right].$$
 (8)

It is easy to prove that this transformation keeps the state $|g\rangle_j|0\rangle$ unaltered, whereas

$$|g\rangle_{j}|1\rangle \longrightarrow |g\rangle_{j}|1\rangle \cos(k\pi/2) - |e_{q}\rangle_{j}|0\rangle ie^{i\phi} \sin(k\pi/2),$$

$$|e\rangle_{j}|0\rangle \longrightarrow |e_{q}\rangle_{j}|0\rangle \cos(k\pi/2) - |g\rangle_{j}|1\rangle ie^{-i\phi} \sin(k\pi/2),$$

where $|0\rangle$ ($|1\rangle$) denotes a state of the CM mode with no (one) phonon.

Let us now show how a two-bit gate can be performed using this interaction. We consider the following three–step process (see Fig. IIB):

- (i) A π laser pulse with polarization q=0 and $\phi=0$ excites the m-th ion. The evolution corresponding to this step is given by $\hat{U}_m^{1,0} \equiv \hat{U}_m^{1,0}(0)$ (Fig. II Ba).
- (ii) The laser directed on the n-th ion is then turned on for a time of a 2π -pulse with polarization q=1 and $\phi=0$. The corresponding evolution operator $\hat{U}_n^{2,1}$ changes the sign of the state $|g\rangle_n|1\rangle$ (without affecting the others) via a rotation through the auxiliary state $|e_1\rangle_n|0\rangle$ (Fig. II Bb).
- (iii) Same as (i).

Thus, the unitary operation for the whole process is $\hat{U}_{m,n} \equiv \hat{U}_m^{1,0} \hat{U}_n^{2,1} \hat{U}_m^{1,0}$ which is represented diagrammatically as follows:

$$\begin{array}{ccccc} & \hat{U}_{m}^{1,0} & \hat{U}_{n}^{2,1} \\ |g\rangle_{m}|g\rangle_{n}|0\rangle & \longrightarrow & |g\rangle_{m}|g\rangle_{n}|0\rangle & \longrightarrow & |g\rangle_{m}|g\rangle_{n}|0\rangle \\ |g\rangle_{m}|e_{0}\rangle_{n}|0\rangle & \longrightarrow & |g\rangle_{m}|e_{0}\rangle_{n}|0\rangle & \longrightarrow & |g\rangle_{m}|e_{0}\rangle_{n}|0\rangle \\ |r_{0}\rangle_{m}|g\rangle_{n}|0\rangle & \longrightarrow & -i|g\rangle_{m}|g\rangle_{n}|1\rangle & \longrightarrow & i|g\rangle_{m}|g\rangle_{n}|1\rangle \\ |e_{0}\rangle_{m}|e_{0}\rangle_{n}|0\rangle & \longrightarrow & -i|g\rangle_{m}|e_{0}\rangle_{n}|1\rangle & \longrightarrow & -i|g\rangle_{m}|r_{0}\rangle_{n}|1\rangle \end{array}$$

$$\begin{array}{lll}
\hat{U}_{m}^{1,0} & & & |g\rangle_{m}|g\rangle_{n}|0\rangle, \\
& \longrightarrow & |g\rangle_{m}|e_{0}\rangle_{n}|0\rangle, \\
& \longrightarrow & |e_{0}\rangle_{m}|g\rangle_{n}|0\rangle, \\
& \longrightarrow & -|e_{0}\rangle_{m}|e_{0}\rangle_{n}|0\rangle.
\end{array} (9)$$

The effect of this interaction is to change the sign of the state only when both ions are initially excited. Note that the state of the CM mode is restored to the vacuum state $|0\rangle$ after the process. Equation (9) is phase gate $|\epsilon_1\rangle|\epsilon_2\rangle \rightarrow (-1)^{\epsilon_1\epsilon_2}|\epsilon_1\rangle|\epsilon_2\rangle$ ($\epsilon_{1,2}=0,1$) which together with single qubit rotations becomes equivalent to a controlled-NOT.

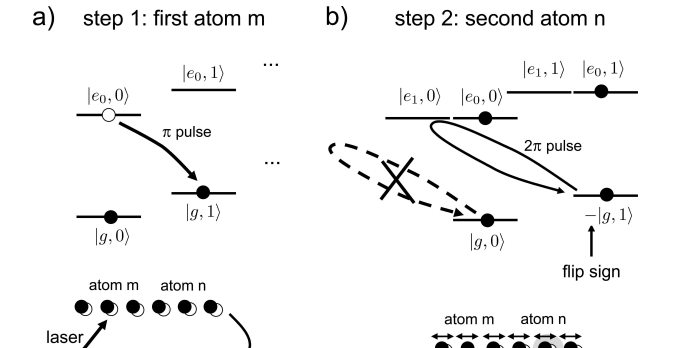


FIG. 2: The two-qubit quantum gate with trapped ions [8]. a) First step according to(9): the qubit of the first atom is swapped to the photonic data bus with a π -pulse on the lower motional sideband, b) Second step: the state $|g,1\rangle$ acquires a minus sign due to a 2π -rotation via the auxiliary atomic level $|r_1\rangle$ on the lower motional sideband.

C. Fast and robust 2-qubit gates for scalable ion trap quantum computing

Scalability of ion trap quantum computing is based on storing a set of ions in a memory area, and moving ions independently to a processing unit: in particular one must bring together pairs of ions to perform a two-qubit gate [16, 17, 18]. Basic steps towards this goal have already been demonstrated experimentally [12]. An important question to be addressed is to identify the current limitations of the two-qubit gates with trapped ions (given the fact that one-qubit gates are significantly simpler with those systems). The ideal scheme should [19]:

- (i) be independent of temperature, so that one does not need to cool the ions to their ground state after they are moved to or from their storage area);
- (ii) require no addressability (to allow the ions to be as close as possible during the gate to increase their interaction strength), and

(iii) be fast, in order to minimize the effects of decoherence during the gate, and to speed up the computation.

This last property has been identified as a key limitation [4]: in essentially all schemes suggested so far [8, 20, 21, 22, 23] one has to resolve spectroscopically the motional sidebands of the ions with the exciting laser, which limits the laser intensity and therefore the gate time. The coherent control-gate gate between pairs of ions [13] analyzed below overcomes this problem by not using spectral methods to couple the ion motion to the internal states but rather mechanical effects.

As our model we consider two ions in a onedimensional harmonic trap, interacting with a laser beam on resonance. The Hamiltonian describing this situation can be written as $H = H_0 + H_1$, where $H_0 = \nu_c a^{\dagger} a + \nu_r b^{\dagger} b$ describes the motion in the trap and

$$H_{1} = \frac{1}{2}\Omega(t) \left[\sigma_{1}^{+} e^{i\eta_{c}(a^{\dagger} + a) + \frac{1}{2}\eta_{r}(b^{\dagger} + b)} + \sigma_{2}^{+} e^{i\eta_{c}(a^{\dagger} + a) - \frac{1}{2}\eta_{r}(b^{\dagger} + b)} \right] + \text{h.c.}$$
(10)

Here, a and b are the annihilation operators center-of-mass and stretching mode, respectively, and $\nu_c = \nu$ and $\nu_r = \sqrt{3}\nu_c$ the corresponding frequencies. We denote by $\eta_c = \eta/\sqrt{2}$ and $\eta_r = \eta\sqrt[4]{4/3}$ are to associated Lamb–Dicke parameters. Note that the Rabi frequency Ω is the same for both ions, i.e. we have not assumed individual addressing.

In the following we will consider two different kind of processes:

- (i) Free evolution, in which the laser is switched off $(\Omega = 0)$ for a certain time;
- (ii) Sequences of pairs of very fast laser pulses, each of them coming from opposite sides, with duration δt long enough to form a π -pulse ($\Omega \delta t = \pi$), but very short compared to the period of the trap ($\nu \delta t \ll 1$).

Processes (i) and (ii) will be alternated: at time t_1 a sequence of z_1 pulses is applied, followed by free evolution until at time t_2 another sequence of z_2 pulses is applied followed by free evolution and so on. The numbers z_k are integers, whose sign indicates the direction of the laser pulses. We can visualize the motion of the ions as a trajectory in phase space. This is illustrated in Fig. 3 for the center-of-mass state of a single ion (X_c, P_c) , where $(X_c + iP_c)/\sqrt{2} = \langle a \rangle$. The time evolution consists of a sequence of kicks (vertical displacements), which are interspersed with free harmonic oscillator evolution (motion along the arcs). The question is now whether we can find a pulse sequence, such that the final phase space point (solid line) is restored to the one corresponding to a free harmonic evolution (dashed circle). In an appendix at the end of this section we show that this can be achieved if the pulse sequence satisfies a commensurability condition for the center-of-mass and stretch-mode

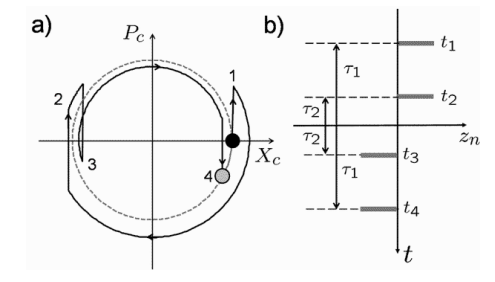


FIG. 3: a) Trajectory in phase space of the center-of-mass state of the ion (X_c, P_c) (where $(X_c + iP_c)/\sqrt{2} = \langle a \rangle$) during the 2-qubit gate (solid line), connecting the initial state (black filled circle) to the final state (grey filled circle) at the gate time T. The time evolution consists of a sequence of kicks (vertical displacements), which are interspersed with free harmonic oscillator evolution (motion along the arcs). A pulse sequence satisfying the commensurability condition (11) guarantees that the final phase space point is restored to the one corresponding to a free harmonic evolution (dashed circle). The particular pulse sequence plotted corresponds to a four pulse sequence given in the text (Protocol I). Figure b) shows how the laser pulses (bars) distribute in time for this scheme.

$$C_c \equiv \sum_{k=1}^{N} z_k e^{-i\nu t_k} = 0, \quad C_r \equiv \sum_{k=1}^{N} z_k e^{-i\sqrt{3}\nu t_k} = 0.$$
 (11)

In this case, the motional state of the ion will not depend on the qubits. Thus the evolution operator is given by (see appendix)

$$\mathcal{U}(\Theta) = e^{i\Theta\sigma_1^z\sigma_2^z} e^{-i\nu_c T a^{\dagger} a} e^{-i\nu_r T b^{\dagger} b}, \tag{12}$$

where T is the total time required by the gate and

$$\Theta = 4\eta^2 \sum_{m=2}^{N} \sum_{k=1}^{m-1} z_k z_m \left[\frac{\sin[\sqrt{3}\nu \Delta t_{km}]}{\sqrt{3}} - \sin(\nu \Delta t_{km}) \right],$$
(13)

is a function of the spacing between laser pulses $\Delta t_{km} = t_k - t_m$. Therefore, if (11) are fulfilled, and $\Theta = \pi/4$ we will produce a controlled–phase gate (which is equivalent to a controlled–NOT gate up to local operations) which is completely independent of the initial motional state, i.e. there are no temperature requirements.

It can be shown [13] that for any value of the time T it is always possible to find a sequence of laser pulses which implements the gate, and therefore the gate operation can be, in principle, arbitrarily fast. We give two simple protocols.

Protocol I: This protocol (see Fig. 3) requires the least number of pulses and produces the gate in a fixed time $T \simeq 1.08(2\pi/\nu)$. The sequence of pulses is defined as

$$(z_n/N, t_n) = \{(\gamma, -\tau_1), (1, -\tau_2), (-1, \tau_2), (-\gamma, \tau_1)\}.$$
(14)

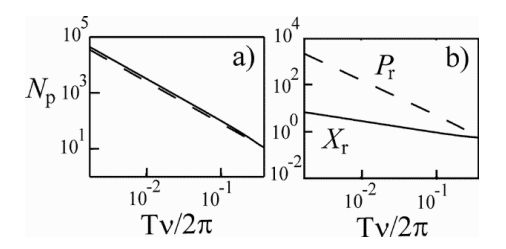


FIG. 4: (a) Log-log plot of the number of pairs of pulses required to produce a phase gate using protocol II, as a function of the duration of the gate, T, for a realistic value[24] of the Lamb–Dicke parameter, $\eta=0.178$. We plot both the exact result (solid line) and a rough estimate $N_P=40(\nu T/2\pi)^{-3/2}$ (dashed line) based on perturbative calculations. (b) Maximum relative displacement, X_r (solid), and maximum momentum acquired, P_r (dashed line), for scheme II. These quantities are dimensionless (scaled) versions of the real observables, $X_r=\max[\langle x_r(t)\rangle/a_0]$, and $P_r\max[\langle p_r(t)\rangle a_0/\hbar]$.

Here $0 < \gamma = \cos(\theta) < 1.0$ is a real number, which may be introduced by tilting both lasers a small angle θ with respect to the axis of the trap, so that no transverse motion is excited. It is always possible to find a solution to Eq. (11) with $\tau_1 \simeq 0.538(4)(2\pi/\nu) > \tau_2 > 0$.

Protocol II: This protocol performs the gate in an arbitrarily short time T. The pulses are now distributed according to

$$(z_n/N, t_n) = \{(-2, -\tau_1), (3, -\tau_2), (-2, -\tau_3) , (2, \tau_3), (-3, \tau_2), (2, \tau_1)\}.$$
(15)

The whole process takes a time $T=2\tau_1$ and requires $N_p=\sum |z_n|=14N$ pairs of pulses. As Fig. 4 shows, the number of pulses increases with decreasing time as $N_p \propto T^{-3/2}$.

Ref. [13] gives a detailed study of the main limitations of the scheme, and provides quantitative estimates for the gate fidelity. On the list of imperfections is first of all anharmonicities of the restoring forces. The more pulses we apply, the larger the relative displacement of the ions, as Fig. 4(b) shows. When the ions become too close to each other, the increasing intensity of the Coulomb force can lead to a breakdown of the harmonic approximation which is implicit in Eq. (10). Imposing an error $E \simeq 10^{-4}$ we estimate the shortest realistic time to be $\nu T \simeq 10^{-3}$ [13]. In addition, laser pulses have a finite duration. However, even for relatively long pulses, we obtain a fidelity which is comparable to the results obtained in current setups [10, 11]. As mentioned before, the scheme is also insensitive to temperature. If the commensurability condition (11) is not perfectly satisfied due to, for example, errors in timing of laser pulses, or misalignment of the lasers, then the corresponding contribution to the gate error is still a weak function of tem-

Finally, we remark that it is not necessary to kick the atoms using pairs of counter-propagating laser beams. The same effect (i.e. a change of sign in η) may also be

achieved in current experiments by reverting the internal state of both ions simultaneously. One then only needs a laser beam (aligned with the trap) to kick the atoms, and another laser (orthogonal to the axis of the trap) to produce the NOT gate. The second and more important remark is that it is possible to avoid errors in the laser pulses by using an adiabatic passage scheme (see references cited in [3]) which is insensitive to fluctuations in the laser intensity. In addition, this method also tolerates that the two ions see slightly different laser intensity.

In summary, the new concept of a "coherent control" two-qubit quantum gate allows operations on a time scale up three orders of magnitude faster than the trap frequency, while at the same time requiring no single ion addressing, no Lamb-Dicke assumption, and ground state cooling of the ion, and being robust against imperfections.

Appendix: Derivation of Eqs. (11) and (12). Here we presents details of the derivation of the commensurability condition (11) to achieve the factorization of the motional states according to Eq. (12). For a pulse sequence, consisting of kicks interspersed with free harmonic time evolution (Fig. 3), we write $\mathcal{U} = \mathcal{U}_c \mathcal{U}_r$, where $\mathcal{U}_{c,r} = \prod_{k=1}^N U_{c,r}(\Delta t_k, z_k)$ has contributions for center-of-mass and relative motion,

$$U_c(t_k, z_k) = e^{-i2z_k\eta_c(a+a^{\dagger})(\sigma_1^z + \sigma_2^z)} e^{-i\nu_c\Delta t_k a^{\dagger} a},$$

$$U_r(t_k, z_k) = e^{-iz_k\eta_r(b+b^{\dagger})(\sigma_1^z - \sigma_2^z)} e^{-i\nu_r\Delta t_k b^{\dagger} b}.$$

The integers z_k indicate the direction of the initial pulse in the sequence of pairs of very fast laser pulses, each of them coming from opposite sites.

In order to fully characterize U, we only have to investigate its action on states of the form $|i\rangle_1|j\rangle_2|\alpha\rangle_c|\beta\rangle_r$, where i,j=0,1 denote the computational basis, and $|\alpha\rangle$ and $|\beta\rangle$ are coherent states. This task can be easily carried out once we know the action of $\mathcal{U}=\prod_{k=1}^N U(\phi_k,p_k)$ on an arbitrary coherent state $|\alpha\rangle$, where

$$U(\phi_k, p_k) = e^{-ip(a+a^{\dagger})} e^{-i\phi_k a^{\dagger} a}.$$

We obtain $\mathcal{U}|\alpha\rangle = e^{i\xi}|\tilde{\alpha}\rangle$, where

$$\tilde{\alpha} = \alpha e^{-i\theta_N} - i \sum_{k=1}^N p_k e^{i(\theta_k - \theta_N)},$$

$$\xi = -\sum_{m=2}^N \sum_{k=1}^{m-1} p_m p_k \sin(\theta_k - \theta_m) - \Re\left[\alpha \sum_{k=0}^N p_k e^{-i\theta_m}\right],$$

with
$$\theta_k = \sum_{m=1}^k \phi_m$$
.

The crucial point is to realize that if $\sum_{k=1}^{N} p_k e^{i\theta_k} = 0$ the motional state $|\alpha\rangle$ after the evolution is the same as if there was only free evolution (Fig. 1a), and a global phase ξ appears which does not depend on the motional state (Fig. 1a). Translating this result to the operators $\mathcal{U}_c|\alpha\rangle$ and $\mathcal{U}_r|\beta\rangle$, we obtain condition (11) for Eq. (12) to be valid.

III. ATOMS IN OPTICAL LATTICES

Bose Einstein condensates (BEC) are a source of a large number of ultracold atoms and, as we will show below, they can also be developed as a tool to provide a large number of qubits stored in optical lattices. In a condensate, due to the weak interactions, all atoms occupy the single particle ground state of the trapping potential, corresponding to a product state of the wave function.

This picture is must be revised by inducing a degeneracy in the ground state which is comparable to the number of atoms. For instance, as first proposed in Refs. [25, 26], it is possible to load a BEC in a deep 3D optical lattice forming a perfect Mott insulator phase with one atom per lattice site. The system is no longer a BEC, but an array of a large number of identifiable qubits, that can be entangled in massively parallel operation with spin-dependent lattices [26]. This scenario has recently been realized in the laboratory in a series of remarkable experiments in Munich [27, 28]. Entanglement of atoms in a lattice can also be achieved by dipole-dipole interactions [29, 30]), and the interactions and the speed of the quantum operations may be significantly enhanced using the very strong interactions are obtained between laser excited Rydberg states [31].

A. Cold atoms in optical lattices: the Hubbard model

Optical lattices are periodic arrays of microtraps for cold atoms generated by standing wave laser fields. The periodic structure of the lattice gives rise to a series of Bloch bands for the atomic center-of-mass motion. Atoms loaded in an optical lattice from a BEC will only occupy the lowest Bloch band due to the low temperatures. The physics of these atoms can be understood in terms of a Hubbard model with Hamiltonian [25]

$$H = -\sum_{\langle i,j\rangle} J_{ij} b_i^{\dagger} b_j + \frac{1}{2} U \sum_i b_i^{\dagger} b_i^{\dagger} b_i b_i . \tag{16}$$

Here b_i and b_i^{\dagger} are bosonic destruction operators for atoms at each lattice site satisfying the bosonic commutation relations $[b_i, b_i^{\dagger}] = \delta_{ij}$. The tunneling of the atoms between different sites is described by the hopping matrix elements J_{ij} . The parameter U is the onsite interaction of atoms resulting from the collisional interactions. The distinguishing feature of this system is the time dependent control of the parameters J_{ij} (kinetic energy) and U (potential energy) by the intensity of the lattice laser. Increasing the intensity of the laser deepens the lattice potential, and suppresses the hopping while at the same time increasing the atomic density at each lattice site and thus the onsite interaction. For shallow lattices $J_{ij} \gg U$ the kinetic energy is dominant, and the ground state of N atoms will be a superfluid in which all bosonic atoms occupy the lowest momentum state

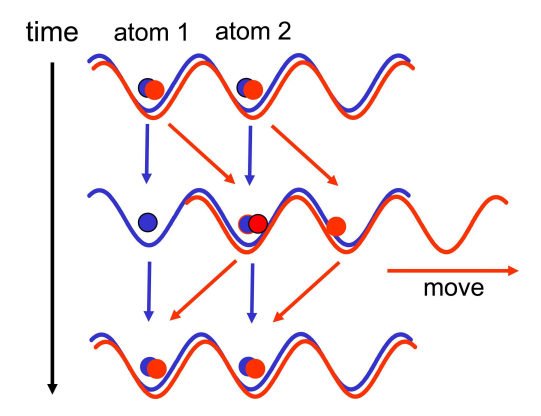


FIG. 5: Controlled collisions of two atoms with internal states $|0\rangle$ and $|1\rangle$ (red and blue circles) in a moveable state-dependent optical lattice (red and blue lattice) to entangle two atoms[26, 28]. This scheme unterlies the quantum simulator on the optical lattice.

in the Bloch band, $(\sum_i b^{\dagger})^N |\text{vac}\rangle$. If $J_{ij} \ll U$, on the other hand, the interactions dominate: for commensurate filling, i.e. when the number of lattice site matches the number of atoms, the ground state becomes a Mottinsulator state $b_1^{\dagger} \dots b_N^{\dagger} |\text{vac}\rangle$ (Fock state of atoms). The superfluid-Mott-insulator transition is an example of a so-called quantum phase transition as studied in Ref. [32]. This Mott insulator regime is of particular interest, as it provides a very large number of identifiable atoms located in the the array of microtraps provided by the optical lattice, whose internal hyperfine or spin states can serve as qubits [25]. The first experimental realization of the Mott insulator quantum phase transition was recently reported by Bloch and collaborators [27].

B. Entanglement via coherent ground state collisions

Entanglement of qubits represented by cold atoms in a Mott-phase can be obtained by combing the collisional interactions (compare the onsite interaction in Eq. 16) with a spin-dependent optical lattice [26]. Let us assume that qubits $|0\rangle$, $|1\rangle$ are stored in two longlived atomic hyperfine ground states. With an appropriate choice of atomic states and the laser configurations [26] we can generate an optical lattice which is spin-dependent, i.e. atoms in $|0\rangle$ and $|1\rangle$ see a different optical potential. In addition these two optical potentials can change in time, so that both lattices have a tunable separation.

This provides us with a mechanism to move atoms conditional to the state of the qubit. In particular, we can collide two atoms "by hand", as illustrated in Fig. 5, so that only the component of the wave function with the first atom in $|1\rangle$ and the second atom in $|0\rangle$ will pick up a collisional phase ϕ , which entangles the atoms. In fact, this interaction gives rise to a phase gate between adjacent atoms $|1\rangle_i|0\rangle_{i+1} \longrightarrow e^{i\phi}|1\rangle_i|0\rangle_{i+1}$. In Fig. 6 we

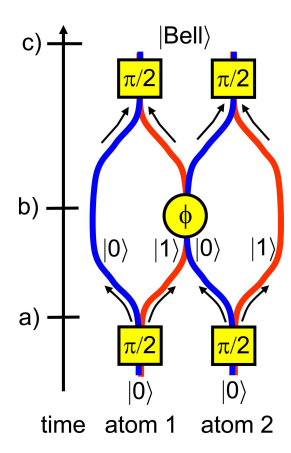


FIG. 6: Ramsey experiment with two atoms colliding in a lattice to generate a Bell state following Ref. [26, 28]. Time evolution is from bottom to top. The two atoms are initially prepared in the product state $|0\rangle|0\rangle$. A $\pi/2$ pulse generates the (unnormalized) superposition state $(|0\rangle+|1\rangle)((|0\rangle+|1\rangle))$ (a). A coherent collision provides a phase shift ϕ conditional to the first atom being in state $|1\rangle$ and the second atom being in state $|0\rangle$, i.e. $|0\rangle|0\rangle+e^{i\phi}|0\rangle|1\rangle+|1\rangle|0\rangle+|1\rangle|1\rangle$ (b). A final $\pi/2$ -pulse closes the Ramsey interferometer resulting in the state $(1-e^{i\phi})|\text{Bell}\rangle+(1+e^{i\phi}|1\rangle|1\rangle$, which for $\phi=\pi$ is a Bell state.

illustrate a Ramsey type experiment to generate and detect a Bell state via these collisional interactions. Again this idea has been demonstrated recently in a seminal experiment in the Munich group[28]. This conditional quantum logic can also be realized with magnetic, electric microtraps and microoptical dipole traps [33, 34, 35].

In more detail, we consider a situation where two atoms with electrons populating the internal states $|0\rangle$ and $|1\rangle$, respectively, are trapped in the ground states $\psi_0^{0,1}$ of two potential wells $V^{0,1}$. Initially, these wells are centered at positions \bar{x}^0 and \bar{x}^1 , sufficiently far apart (distance $d = \bar{x}_1 - \bar{x}_0$) so that the particles do not interact. The positions of the potentials are moved along trajectories $\bar{x}^0(t)$ and $\bar{x}^1(t)$ so that the wavepackets of the atoms overlap for certain time, until finally they are restored to the initial position at the final time. This situation is described by the Hamiltonian

$$H = \sum_{\beta=0,1} \left[\frac{(\hat{p}^{\beta})^2}{2m} + V^{\beta} \left(\hat{x}^{\beta} - \bar{x}^{\beta}(t) \right) \right] + u^{01} (\hat{x}^0 - \hat{x}^1). \tag{17}$$

Here, $\hat{x}^{0,1}$ and $\hat{p}^{0,1}$ are position and momentum operators, $V^{0,1}\left(\hat{x}^{0,1}-\bar{x}^{0,1}(t)\right)$ describe the displaced trap potentials and u^{01} is the atom–atom interaction term. Ideally, we would like to implement the transformation from before to after the collision,

$$\psi^0_0(x^0-\bar{x}^0)\psi^1_0(x^b-\bar{x}^1) \rightarrow e^{i\phi}\psi^0_0(x^0-\bar{x}^0)\psi^1_0(x^1-\bar{x}^1), \ (18)$$

where each atom remains in the ground state of its trapping potential and preserves its internal state. The phase ϕ will contain a contribution from the interaction (collision). The transformation (18) can be realized in the

adiabatic limit, whereby we move the potentials slowly on the scale given by the trap frequency, so that the atoms remain in the ground state. Moving non-interacting atoms will induce kinetic single particle kinetic phases. In the presence of interactions ($u^{ab} \neq 0$), we define the time–dependent energy shift due to the interaction as

$$\Delta E(t) = \frac{4\pi a_s \hbar^2}{m} \int dx |\psi_0^0 \left(x - \bar{x}^0(t) \right)|^2 |\psi_0^1 \left(x - \bar{x}^1(t) \right)|^2, \tag{19}$$

where a_s is the s-wave scattering length. We assume that $|\Delta E(t)| \ll \hbar \nu$ with ν the trap frequency so that no sloshing motion is excited. In this case, (18) still holds with $\phi = \phi^0 + \phi^1 + \phi^{01}$, where in addition to (trivial) single particle kinetic phases ϕ^0 and ϕ^1 arising from moving the potentials, we have a collisional phase shift

$$\phi^{01} = \int_{-\infty}^{\infty} dt \Delta E(t) / \hbar. \tag{20}$$

If the first atom is in a superposition state of the two qubits, the atomic wave packet would be "split" by moving the state dependent potentials, very much like with a beam splitter in atom interferometry. Thus we can move the potentials of neighboring atoms such that only the $|0\rangle$ component of the first atom "collides" with the state $|0\rangle$ of the second atom

$$|0\rangle_{1}|0\rangle_{2} \to e^{i2\phi^{0}}|0\rangle_{1}|0\rangle_{2},$$

$$|0\rangle_{1}|1\rangle_{2} \to e^{i(\phi^{0}+\phi^{1}+\phi^{01})}|0\rangle_{1}|1\rangle_{2},$$

$$|1\rangle_{1}|0\rangle_{2} \to e^{i(\phi^{0}+\phi^{1})}|b\rangle_{1}|0\rangle_{2},$$

$$|1\rangle_{1}|1\rangle_{2} \to e^{i2\phi^{1}}|1\rangle_{1}|1\rangle_{2},$$
(21)

where the motional states remain unchanged in the adiabatic limit, and ϕ^0 and ϕ^1 are single particle kinetic phases. The transformation (21) corresponds to a fundamental two–qubit gate. The fidelity of this gate is limited by nonadiabatic effects, decoherence due to spontaneous emission in the optical potentials and collisional loss to other unwanted states, or collisional to unwanted states. According to Ref. [26] the fidelity of this gate operation is remarkably close to one in a large parameter range.

C. Application: quantum simulations

Applying the previous method to an optical lattice that has more qubits, we can entangle many atoms with a single lattice movement, i.e. in a highly parallel entanglement operation. While for two atoms we have obtained a Bell state (see Fig. 6), for three atoms this produces a maximally entangled GHZ-state, and for 2D lattices this allows the generation of a cluster state, which is the basic resource for universal quantum computing in Briegel et al.'s one way quantum computer[36].

The parallelism inherent in the lattice movements makes "atoms in optical lattices" an ideal candidate for

a Feynman-type quantum simulator (see the Appendix of this section) for bosonic, fermionic and spin many body systems, allowing simulation of various types and strengths of particle interactions, and 1, 2 or 3D lattice configurations in a regime of many atoms, clearly unaccessible to any classical computer. By a stroboscopic switching of laser pulses and lattice movements combined with collisional interactions one can implement sequences of 1 and 2-qubit operations to simulate the time evolution operator of a many body system [37]. For translationally invariant systems, there is no need to address individual lattice sites, which makes the requirements guite realistic in the light of the present experimental developments. On the other hand, as noted above, Hubbard Hamiltonians with interactions controlled by lasers can also be realized directly with cold bosonic or fermionic atoms in optical lattices. This "analogue" quantum simulation provides a direct way of studying properties of strongly correlated systems in cold atom labs, which in the future may develop into a novel tool of condensed matter physics.

For the near future, we expect that atoms in optical lattices will be used to simulate a variety of other physical systems like, for example, interacting Fermions in 2 Dimensions using different lattice geometries. We also expect an important progress towards loading single (neutral) atoms in different types of potentials (optical, magnetic, etc), and the performance of quantum gates with few of these systems. This would allow to create few atom entangled states which may be used to observe violations of Bell inequalities, or to observe interesting phenomena like teleportation or error correction. As opposed to the trapped ions, at the moment it is hard to predict whether scalable quantum computation will be possible with neutral atoms in optical lattices using the present experimental set-ups. In any case, due to the high parallelism of these systems, we can clearly foresee that they will allow us to obtain a very deep insight in condensed matter physics via quantum simulations.

Appendix: Quantum simulator In brief, the basic concept of the quantum simulator is as follows. Let us consider a quantum system composed of N qubits all initially in state $|0\rangle$. We apply a two-qubit gate (specified by a 4×4 unitary matrix) to the first and second qubit, another one to the second and the third, and so on until we have performed N-1 such gates. Now, we measure the last qubit in the basis $|0\rangle, |1\rangle$. Let us denote by p_0 and p_1 the probability of obtaining 0 and 1 in this measurement. Our goal is to determine such probabilities with a prescribed precision (for example, of 1%). A way to determine the probabilities using a classical computer is to simulate the whole process: we take a vector which has 2^N components and multiply it by a $2^N \times 2^N$ matrix every time we simulate the action of a gate. At the end we can calculate the desired probabilities using the standard rules of Quantum Mechanics. However, as soon as N is of the order of 30, we will not be able to store the vector and the matrices in any existing computer. Moreover,

the time required to simulate the action of the gates will increase exponentially with the number of gubits. However, with a quantum computer this simulation will required to repeat the same computation of the order of 100 times, and each computation requires only N-1 gates. Thus, we see that the quantum computer itself is much more efficient to simulate quantum systems, something that Feynman already pointed out in 1982 [1, 38]. Of course, this particular example is artificial, and it is not related to a real problem. However, there exist physical systems which cannot be simulated with classical computers but in which a quantum computer could offer an important insight on some physical phenomena which are not yet understood [38]. For example, one could use a quantum computer to simulate spin systems or Hubbard models, and extract some information about open questions in condensed matter physics. Another possibility is to use an "analogue" quantum computer (as our artificial Hubbard models) to do the job, i.e. to choose a system which is described by the same Hamiltonian which one wants to simulate, but that can be very well controlled and measured.

IV. QUANTUM INFORMATION PROCESSING WITH ATOMIC ENSEMBLES

A. Introduction

In the previous section, the quantum computation schemes are based on laser manipulation of single trapped particles. Here, we will show that laser manipulation of macroscopic atomic ensembles can also be exploited for implementation of quantum information processing [39, 40, 41, 42, 43, 44, 45, 46, 47, 48]. In particular, we will discuss the uses of this system for continuous variable quantum teleportation and for implementation of quantum repeaters which enable scalable long-distance quantum communication.

The atomic ensemble contains a large number of identical neutral atoms, whose experimental candidates can be either laser-cooled atoms [46, 49, 50], or room-temperature gas [44, 47, 48, 51, 52]. The motivation of using atomic ensembles instead of single-particles for quantum information processing is mainly two-folds: firstly, laser manipulation of atomic ensembles without separate addressing of individual atoms is typically much easier than the laser manipulation of single particles; secondly and more importantly, the use of the atomic ensembles allows for some collective effects resulting from many-atom coherence to enhance the signal-to-noise ratio, which is critical for implementations of some quantum information protocols.

In the next section, we first show the ideas of using atomic ensembles for implementation of scalable long-distance quantum communication. Long-distance quantum communication is necessarily based on the use of photonic channels. However, due to losses and decoher-

ence in the channel, the communication fidelity decreases exponentially with the channel length. To overcome this outstanding problem, one needs to use the concept of quantum repeaters [53], which provide the only known way for robust long-distance quantum communication. The best known method for complete implementation of quantum repeaters with sensible experimental technologies was proposed in Ref. [40]. Significant experimental advances haven been achieved recently towards realization of this comprehensive scheme, and we will briefly review these advances. In the final section, we discuss the use of atomic ensembles for continuous variable quantum information processing. Laser manipulation of atomic ensembles provides an elegant way for realizing continuous variable atomic quantum teleportation [42], and we will review the basic theoretical schemes as well as the following experimental achievements.

B. Atomic ensembles for implementation of quantum repeaters

Quantum communication is an essential element required for constructing quantum networks and for secretly transferring messages by means of quantum cryptography. The central problem of quantum communication is to generate nearly perfect entangled states between distant sites. Such states can be used then to implement secure quantum cryptography [54] or to transfer arbitrary quantum messages [55]. The schemes for quantum communication need to be based on the use of the photonic channels. To overcome the inevitable signal attenuation in the channel, the concept of entanglement purification was invented [56]. However, entanglement purification does not fully solve the problem for long-distance quantum communication. Due to the exponential decay of the entanglement in the channel, one needs an exponentially large number of partially entangled states to obtain one highly entangled state, which means that for a sufficiently long distance the task becomes nearly impossible.

The idea of quantum repeaters was proposed to solve the difficulty associated with the exponential fidelity decay [53]. In principle, it allows to make the overall communication fidelity very close to the unity, with the communication time growing only polynomially with the transmission distance. In analogy to fault-tolerant quantum computing [57], the quantum repeater proposal is a concatenated entanglement purification protocol for communication systems. The basic idea is to divide the transmission channel into many segments, with the length of each segment comparable to the channel attenuation length. First, one generates entanglement and purifies it for each segment; the purified entanglement is then extended to a longer length by connecting two adjacent segments through entanglement swapping [55]. After entanglement swapping, the overall entanglement is decreased, and one has to purify it again. One can continue the rounds of the entanglement swapping and purification until a nearly perfect entangled states are created between two distant sites.

To implement the quantum repeater protocol, one needs to generate entanglement between distant quantum bits (qubits), store them for sufficiently long time and perform local collective operations on several of these qubits. The requirement of quantum memory is essential since all purification protocols are probabilistic. When entanglement purification is performed for each segment of the channel, quantum memory can be used to keep the segment state if the purification succeeds and to repeat the purification for the segments only where the previous attempt fails. This is essentially important for polynomial scaling properties of the communication efficiency since with no available memory we have to require that the purifications for all the segments succeeds at the same time; the probability of such event decreases exponentially with the channel length. The requirement of quantum memory implies that we need to store the local qubits in the atomic internal states instead of the photonic states since it is difficult to store photons for a reasonably long time. With atoms as the local information carriers it seems to be very hard to implement quantum repeaters since normally one needs to achieve the strong coupling between atoms and photons with high-finesse cavities for atomic entanglement generation, purification, and swapping [58, 59], which, in spite of the recent significant experimental advances [60, 61, 62, 63], remains a very challenging technology.

To overcome this difficulty, a scheme was proposed in Ref. [40] to realize quantum repeaters based on the use of atomic ensembles. The laser manipulation of the atomic ensembles, together with simple linear optics devices and routine single-photon detection, do the whole work for long-distance quantum communication. This scheme combines entanglement generation, connection, and application, with built-in entanglement purification, and as a result, it is inherently resilient to influence of noise and imperfections. Here, we will first explain the basic ideas of this theoretical proposal and then review the recent experimental advances.

1. Entanglement generation

To realize long-distance quantum communication, first we need to entangle two atomic ensembles within the channel attenuation length. This entanglement generation scheme is based on single-photon interference at photodetectors, which critically uses the fault-tolerance property of the photon detection [64] and the collective enhancement of the signal-to-noise ratio available in a many-atomic ensemble under an appropriate interaction configuration [65].

The system is a sample of atoms prepared in the ground state $|1\rangle$ with the level configuration shown in Fig. IV B 1. This sample is illuminated by a short,

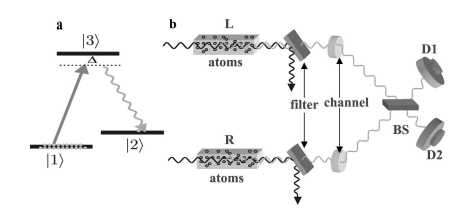


FIG. 7: (a) The relevant level structure of the atoms in the ensemble with $|1\rangle$, the ground state, $|2\rangle$, the metastable state for storing a qubit, and $|3\rangle$, the excited state. The transition $|1\rangle \rightarrow |3\rangle$ is coupled by the classical laser with the Rabi frequency Ω , and the forward scattering Stokes light comes from the transition $|3\rangle \rightarrow |2\rangle$. For convenience, we assume off-resonant coupling with a large detuning Δ . (b) Schematic setup for generating entanglement between the two atomic ensembles L and R. The two ensembles are pencil shaped and illuminated by the synchronized classical laser pulses. The forward-scattering Stokes pulses are collected after the filters (polarization and frequency selective) and interfered at a 50%-50% beam splitter BS after the transmission channels, with the outputs detected respectively by two single-photon detectors D1 and D2. If there is a click in D1 or D2, the process is finished and we successfully generate entanglement between the ensembles L and R. Otherwise, we first apply a repumping pulse to the transition $|2\rangle \rightarrow |3\rangle$ on the ensembles L and R to set the state of the ensembles back to the ground state $|0\rangle_a^L \otimes |0\rangle_a^R$, then the same classical laser pulses as the first round are applied to the transition $|1\rangle \rightarrow |3\rangle$ and we detect again the forward-scattering Stokes pulses after the beam splitter. This process is repeated until finally we have a click in the D1 or D2 detector.

off-resonant laser pulse that induces Raman transitions into the state $|2\rangle$ (a hyperfine level in the ground-state manifold with a long coherence time). We are particularly interested in the forward-scattered Stokes light that is co-propagating with the laser. Such scattering events are uniquely correlated with the excitation of the symmetric collective atomic mode S given by $S \equiv \left(1/\sqrt{N_a}\right) \sum_i |g\rangle_i \langle s|$ [65], where the summation is taken over all the atoms. In particular, an emission of the single Stokes photon in a forward direction results in the state of atomic ensemble given by $S^{\dagger}|0_a\rangle$, where the ensemble ground state $|0_a\rangle \equiv \bigotimes_i |1\rangle_i$.

We assume that the light-atom interaction time is short so that the mean photon number in the forward-scattered Stokes pulse is much smaller than 1. One can assign an effective single-mode bosonic operator a for this Stokes pulse with the corresponding vacuum state denoted by $|0_p\rangle$. The whole state of the atomic collective mode and the forward-scattered Stokes mode can now be written in the following form [65]

$$|\phi\rangle = |0_a\rangle |0_p\rangle + \sqrt{p_c}S^{\dagger}a^{\dagger} |0_a\rangle |0_p\rangle + o(p_c), \qquad (22)$$

where p_c is the small excitation probability.

Now we explain how to use this setup to generate entanglement between two distant ensembles L and R us-

ing the configuration shown in Fig. IVB1. Here, two laser pulses excited both ensembles simultaneously, and the whole system is described by the state $|\phi\rangle_L \otimes |\phi\rangle_R$, where $|\phi\rangle_L$ and $|\phi\rangle_R$ are given by Eq. (22) with all the operators and states distinguished by the subscript L or R. The forward scattered Stokes signal from both ensembles is combined at the beam splitter and a photodetector click in either D1 or D2 measures the combined radiation from two samples, $a_{+}^{\dagger}a_{+}$ or $a_{-}^{\dagger}a_{-}$ with $a_{\pm} = (a_L \pm e^{i\varphi} a_R)/\sqrt{2}$. Here, φ denotes an unknown difference of the phase shifts in the two-side channels. We can also assume that φ has an imaginary part to account for the possible asymmetry of the setup, which will also be corrected automatically in our scheme. But the setup asymmetry can be easily made very small, and for simplicity of expressions we assume that φ is real in the following. Conditional on the detector click, we should apply a_+ or a_- to the whole state $|\phi\rangle_L \otimes |\phi\rangle_R$, and the projected state of the ensembles L and R is nearly maximally entangled with the form (neglecting the high-order terms $o(p_c)$

$$|\Psi_{\varphi}\rangle_{LR}^{\pm} = \left(S_L^{\dagger} \pm e^{i\varphi} S_R^{\dagger}\right)/\sqrt{2} \left|0_a\right\rangle_L \left|0_a\right\rangle_R. \tag{23}$$

The probability for getting a click is given by p_c for each round, so we need repeat the process about $1/p_c$ times for a successful entanglement preparation, and the average preparation time is given by $T_0 \sim t_\Delta/p_c$. The states $|\Psi_r\rangle_{LR}^+$ and $|\Psi_r\rangle_{LR}^-$ can be easily transformed to each other by a simple local phase shift. Without loss of generality, we assume in the following that we generate the entangled state $|\Psi_r\rangle_{LR}^+$.

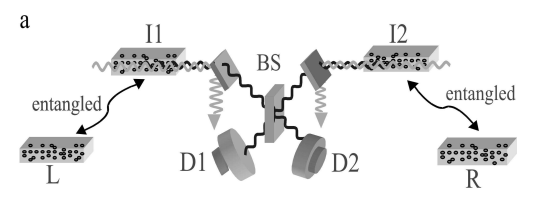
The presence of noise will modify the projected state of the ensembles to

$$\rho_{LR}\left(c_{0},\varphi\right) = \frac{1}{c_{0}+1} \left(c_{0}\left|0_{a}0_{a}\right\rangle_{LR}\left\langle0_{a}0_{a}\right| + \left|\Psi_{\varphi}\right\rangle_{LR}^{+}\left\langle\Psi_{\varphi}\right|\right),\tag{24}$$

where the "vacuum" coefficient c_0 is determined by the dark count rates of the photon detectors. It will be seen below that any state in the form of Eq. (24) will be purified automatically to a maximally entangled state in the entanglement-based communication schemes. We therefore call this state an effective maximally entangled (EME) state with the vacuum coefficient c_0 determining the purification efficiency.

2. Entanglement connection through swapping

After successful generation of entanglement within the attenuation length, we want to extend the quantum communication distance. This is done through entanglement swapping with the configuration shown in Fig. IV B 2. Suppose that we start with two pairs of the entangled ensembles described by the state $\rho_{LI_1} \otimes \rho_{I_2R}$, where ρ_{LI_1} and ρ_{I_2R} are given by Eq. (24). In the ideal case, the setup shown in Fig. IV B 2 measures the quantities corresponding to operators $S_{\pm}^{\dagger}S_{\pm}$ with $S_{\pm}=(S_{I_1}\pm S_{I_2})/\sqrt{2}$.



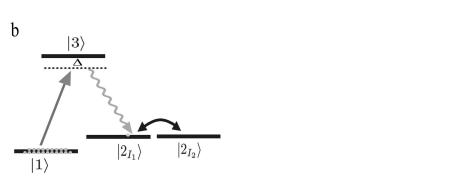


FIG. 8: (a) Illustrative setup for the entanglement swapping. We have two pairs of ensembles L, I₁ and I₂, R distributed at three sites L, I and R. Each of the ensemble-pairs L, I₁ and I₂, R is prepared in an EME state in the form of Eq. (3). The excitations in the collective modes of the ensembles I₁ and I₂ are transferred simultaneously to the optical excitations by the repumping pulses applied to the atomic transition $|2\rangle \rightarrow |3\rangle$, and the stimulated optical excitations, after a 50%-50% beam splitter, are detected by the singlephoton detectors D1 and D2. If either D1 or D2 clicks, the protocol is successful and an EME state in the form of Eq. (3) is established between the ensembles L and R with a doubled communication distance. Otherwise, the process fails, and we need to repeat the previous entanglement generation and swapping until finally we have a click in D1 or D2, that is, until the protocol finally succeeds. (b) The two intermediated ensembles I₁ and I₂ can also be replaced by one ensemble but with two metastable states I₁ and I₂ to store the two different collective modes. The 50%-50% beam splitter operation can be simply realized by a $\pi/2$ pulse on the two metastable states before the collective atomic excitations are transferred to the optical excitations.

If the measurement is successful (i.e., one of the detectors registers one photon), we will prepare the ensembles L and R into another EME state. The new φ -parameter is given by $\varphi_1 + \varphi_2$, where φ_1 and φ_2 denote the old φ -parameters for the two segment EME states. Even in the presence of realistic noise such as the photon loss, an EME state is still created after a detector click. The noise only influences the success probability to get a click and the new vacuum coefficient in the EME state. The above method for connecting entanglement can be continued to arbitrarily extend the communication distance.

3. Entanglement-based communication schemes

After an EME state has been established between two distant sites, we would like to use it in the communication protocols, such as for quantum teleportation, cryptography, or Bell inequality detection. It is not obvious that the EME state (24), which is entangled in the Fock basis,

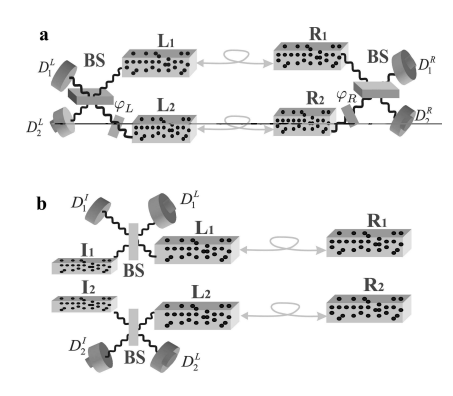


FIG. 9: (a) Schematic setup for the realization of quantum cryptography and Bell inequality detection. Two pairs of ensembles L₁, R₁ and L₂, R₂ have been prepared in the EME states. The collective atomic excitations on each side are transferred to the optical excitations, which, respectively after a relative phase shift φ_L or φ_R and a 50%-50% beam splitter, are detected by the single-photon detectors D_1^L, D_2^L and D_1^R, D_2^R . We look at the four possible coincidences of D_1^R, D_2^R with D_1^L, D_2^L , which are functions of the phase difference $\varphi_L - \varphi_R$. Depending on the choice of φ_L and φ_R , this setup can realize both the quantum cryptography and the Bell inequality detection. (b) Schematic setup for probabilistic quantum teleportation of the atomic "polarization" state. Similarly, two pairs of ensembles L₁, R₁ and L₂, R₂ are prepared in the EME states. We want to teleport an atomic "polarization" state $\left(d_0S_{I_1}^{\dagger}+d_1S_{I_2}^{\dagger}\right)\left|0_a0_a\right\rangle_{I_1I_2}$ with unknown coefficients d_0, d_1 from the left to the right side, where $S_{I_1}^{\dagger}, S_{I_2}^{\dagger}$ denote the collective atomic operators for the two ensembles I_1 and I_2 (or two metastable states in the same ensemble). The collective atomic excitations in the ensembles I_1 , L_1 and I₂, L₂ are transferred to the optical excitations, which, after a 50%--50% beam splitter, are detected by the single-photon detectors D_1^I , D_1^L and D_2^I , D_2^L . If there are a click in D_1^I or D_1^L and a click in D_2^I or D_2^I , the protocol is successful. A π -phase rotation is then performed on the collective mode of the ensemble R_2 conditional on that the two clicks appear in the detectors D_1^I, D_2^L or D_2^I, D_1^L . The collective excitation in the ensembles R₁ and R₂, if appearing, would be found in the same "polarization" state $\left(d_0S_{R_1}^\dagger + d_1S_{R_2}^\dagger\right)|0_a0_a\rangle_{R_1R_2}$.

is useful for these tasks since in the Fock basis it is experimentally hard to do certain single-bit operations. In the following we will show how the EME states can be used to realize all these protocols with simple experimental configurations.

Quantum cryptography and the Bell inequality detection are achieved with the setup shown by Fig. IV B 3a. The state of the two pairs of ensembles is expressed as $\rho_{L_1R_1}\otimes\rho_{L_2R_2}$, where $\rho_{L_iR_i}$ (i=1,2) denote the same EME state with the vacuum coefficient c_n if we have done n times entanglement connection. The φ -parameters in $\rho_{L_1R_1}$ and $\rho_{L_2R_2}$ are the same provided that the two states are established over the same stationary channels. We register only the coincidences of the two-side detec-

tors, so the protocol is successful only if there is a click on each side. Under this condition, the vacuum components in the EME states, together with the state components $S_{L_1}^{\dagger} S_{L_2}^{\dagger} |\text{vac}\rangle$ and $S_{R_1}^{\dagger} S_{R_2}^{\dagger} |\text{vac}\rangle$, where $|\text{vac}\rangle$ denotes the ensemble state $|0_a 0_a 0_a 0_a \rangle_{L_1 R_1 L_2 R_2}$, have no contributions to the experimental results. So, for the measurement scheme shown by Fig. IV B1, the ensemble state $\rho_{L_1 R_1} \otimes \rho_{L_2 R_2}$ is effectively equivalent to the following "polarization" maximally entangled (PME) state (the terminology of "polarization" comes from an analogy to the optical case)

$$|\Psi\rangle_{\rm PME} = \left(S_{L_1}^{\dagger} S_{R_2}^{\dagger} + S_{L_2}^{\dagger} S_{R_1}^{\dagger}\right) / \sqrt{2} |\text{vac}\rangle.$$
 (25)

The success probability for the projection from $\rho_{L_1R_1} \otimes \rho_{L_2R_2}$ to $|\Psi\rangle_{\rm PME}$ (i.e., the probability to get a click on each side) is given by $p_a = 1/[2\,(c_n+1)^2]$. One can also check that in Fig. IVB3, the phase shift ψ_{Λ} ($\Lambda = L$ or R) together with the corresponding beam splitter operation are equivalent to a single-bit rotation in the basis $\left\{|0\rangle_{\Lambda} \equiv S_{\Lambda_1}^{\dagger}\,|0_a0_a\rangle_{\Lambda_1\Lambda_2}\,,\,\,|1\rangle_{\Lambda} \equiv S_{\Lambda_2}^{\dagger}\,|0_a0_a\rangle_{\Lambda_1\Lambda_2}\right\}$ with the rotation angle $\theta = \psi_{\Lambda}/2$. Since we have the effective PME state and we can perform the desired single-bit rotations in the corresponding basis, it is clear how to use this facility to realize quantum cryptography, Bell inequality detection, as well as teleportation (see Fig. IV B 3b).

It is remarkable that all the steps of entanglement generation, connection, and applications described above are robust to practical noise. The dominant noise in this system is photon loss, including the contributions from the channel attenuation, the detector and the coupling inefficiencies etc. It the photon is lost, we will never get a click from the detectors, and we simply repeat this failed attempt until we succeed. So this noise only influences the efficiency to register a photon, but has no influence on the final state fidelity if the photon is registered. Furthermore, one can show that the nose influence on the efficiency is actually only moderate in the sense that the required number of attempts for a successful event only increases with the communication distance by a slow polynomial law [40]. So we get high-fidelity quantum communication with a moderate polynomial overhead, which is the essential advantage of the quantum repeater protocol.

4. Recent experimental advances

The physics behind the above scheme for quantum repeaters is based on the definite correlation between the forward-scattered Stokes photon and the long-lived excitation in the collective atomic mode. The correlation comes from the collective enhancement effect due to many-atom coherence (for a single atom, the atomic excitation cannot be correlated with radiation in a certain

direction without the use of high-finesse cavities [65]). The entanglement generation, connection, and application schemes described above are all based on this correlation. So the first enabling step for demonstration of this comprehensive quantum repeater scheme is to verify this correlation. Several exciting experiments have been reported on demonstration of this correlation effect [46, 47, 48].

The first experiment was reported from Caltech which demonstrate the non-classical correlation between the emitted photon and the collective atomic excitation. The collective atomic excitation is subsequently transferred to a forward-scattered anti-Stokes photon for measurements (see Sec. 3.2.2), so what one really detects in experiments is the correlation between the pair of Stokes and anti-Stokes photons emitted successively. In the Caltech experiment, the atomic ensemble is a cloud of cold atomic in a magnetic optical trap. To experimentally confirm the correlation between the Stokes and the anti-Stokes photons, one measures the auto-correlations $\tilde{g}_{1,1}, \tilde{g}_{2,2}$ of the Stokes and the anti-Stokes fields and the cross correlation $\tilde{g}_{1,2}$ between them. For any classical optical fields (fields with well defined P-representations), these correlations should satisfy the Cauthy-Schwarz inequality $[\tilde{g}_{1,2}]^2 \leq \tilde{g}_{1,1}\tilde{g}_{2,2}$, while for correlations between the non-classical single-photon pairs, this inequality will be violated. In the experiment [46], this inequality was measured to be strongly violated with $[\tilde{g}_{1,2}^2(\delta t)]$ 5.45 ± 0.11] $\nleq [\tilde{g}_{1,1}\tilde{g}_{2,2} = 2.97 \pm 0.08]$. Here, δt is the time delay between the pair of Stokes and anti-Stokes photons, which is 405 ns in the initial experiment but could be much longer (up to seconds) if one loads the atoms into a far-off-resonant optical trap. Note that δt is basically limited by the spin relaxation time in the ensemble, and for implementation of quantum repeaters it is important to get a long δt to enable storage of quantum information in the ensemble.

Another related experiment was reported from Harvard [47], which uses hot atomic gas instead of the cold atomic ensemble. This experiment also measures the correlation between the Stokes and anti-Stokes fields. The difference is that it is not operated in the single-photon region. Instead, both the Stokes and anti-Stokes fields may have up to thousand of photons. In this limit, there is also some inequality need to be satisfied by the classical fields, and the experiment measures a violation of this inequality by about 4%. The other experiment with roomtemperature atomic gas was reported from USTC [48], which operates in the single-photon region as required by the quantum repeater scheme. This experiment uses a similar detection method as the Caltech experiment, and measures a violation of the Cauchy-Schwarz inequality with $\left[g_{1,2}^2(\delta t) = 4.17 \pm 0.09\right] \nleq \left[g_{1,1}g_{2,2} = 3.12 \pm 0.08\right],$ where the time delay δt is observed to be about 2 μ s.

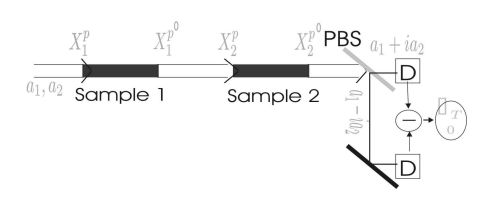


FIG. 10: Schematic setup for Bell measurements. A linearly polarized strong laser pulse (decomposed into two circular polarization modes a_1, a_2) propagates successively through the two atomic samples. The two polarization modes $(a_1 + ia_2)/\sqrt{2}$ and $(a_1 - ia_2)/\sqrt{2}$ are then split by a polarizing beam splitter (PBS), and finally the difference of the two photon currents (integrated over the pulse duration T) is measured.

C. Atomic ensembles for continuous variable quantum information processing

In continuous variable quantum information protocols, information is carried by some observables with continuous values. There have been quite a lot of interests in continuous variable information processing, including proposals for continuous variable quantum teleportation, cryptography, computation, error correction, and entanglement purification [2].

Here we will review some recent schemes using atomic ensembles for realization of continuous variable quantum teleportation [41, 42, 44]. Note that atomic quantum teleportation (not realized yet) typically requires strong coupling between the atom and the photon. Collective enhancement in the atomic ensemble plays an important role here as it significantly alleviates this stringent requirement. We will briefly explain the idea in Ref. [42] which uses only coherent light to generate continuous variable entanglement between two distant ensembles for atomic quantum teleportation. The scheme in [42] has been followed by the exciting experiment reported in Ref. [44] which demonstrates entanglement between two macroscopic ensembles for the first time.

For an optical field with two circular polarization modes $a_1,\ a_2,$ one can introduce the Stokes operators by $S_x^p = \frac{1}{2} \left(a_1^\dagger a_2 + a_2^\dagger a_1 \right),\ S_y^p = \frac{1}{2i} \left(a_1^\dagger a_2 - a_2^\dagger a_1 \right),$ $S_z^p = \frac{1}{2} \left(a_1^\dagger a_1 - a_2^\dagger a_2 \right).$ If the light is linearly polarized along the $\overrightarrow{x'}$ direction, one can define a pair of canonical operators by $X^p = S_y^p / \sqrt{\langle S_x^p \rangle},\ P^p = S_z^p / \sqrt{\langle S_x^p \rangle}$ with $[X^p,P^p]=i.$ Similarly, for a polarized atomic ensemble with the collective spin $\overrightarrow{S^a}$ pointing to the $\overrightarrow{x'}$ direction, one can also define a pair of canonical operators $X^a = S_y^a / \sqrt{\langle S_x^a \rangle},\ P^a = S_z^a / \sqrt{\langle S_x^a \rangle}$ with $[X^a,P^a]=i.$ When the light passes through the atomic ensemble in an appropriate off-resonant interaction configuration detailed in Ref. [42], the continuous variable operators defined above will transform by the following form

$$X^{p\prime} = X^p - \kappa_c P^a,$$

$$X^{a\prime} = X^a - \kappa_c P^p,$$

$$P^{\beta\prime} = P^\beta, \quad (\beta = a, p),$$
(26)

where κ_c is a parameter characterizing the interaction strength whose typical value is around 5.

For quantum teleportation, first one needs to generate entanglement between two distant ensembles 1 and 2. This is done through a nonlocal Bell measurement of the EPR operators $X_1^a - X_2^a$ and $P_1^a + P_2^a$ with the setup depicted by Fig. IVC. This setup measures the Stokes operator $X_2^{p'}$ of the output light. Using Eq. (3.5), we have $X_2^{p'} = X_1^p + \kappa_c (P_1^a + P_2^a)$, so we get a collective measurement of $P_1^a + P_2^a$ with some inherent vacuum noise X_1^p . The efficiency $1 - \eta$ of this measurement is determined by the parameter κ_c with $\eta = 1/(1+2\kappa_c^2)$. After this round of measurements, we rotate the collective atomic spins around the x axis to get the transformations $X_1^a \to -P_1^a$, $P_1^a \to X_1^a$ and $X_2^a \to P_2^a$, $P_2^a \to -X_2^a$. The rotation of the atomic spin can be easily obtained by applying classical laser pulses. After the rotation, the measured observable of the first round of measurement is changed to $X_1^a - X_2^a$ in the new variables. We then make another round of collective measurement of the new variable $P_1^a + P_2^a$. In this way, both the EPR operators $X_1^a - X_2^a$ and $P_1^a + P_2^a$ are measured, and the final state of the two atomic ensembles is collapsed into a two-mode squeezed state with variance $\delta \left(X_1^a-X_2^a\right)^2=\delta \left(P_1^a+P_2^a\right)^2=e^{-2r}$, where the squeezing parameter r is given by

$$r = \frac{1}{2} \ln \left(1 + 2\kappa_c^2 \right). \tag{27}$$

Thus, using only coherent light, we generate continuous variable entanglement [66] between two nonlocal atomic ensembles. With the interaction parameter $\kappa_c \approx 5$, a high squeezing (and thus a large entanglement) $r \approx 2.0$ is obtainable.

To achieve quantum teleportation, first the ensembles 1 and 2 are prepared in a continuous variable entangled state using the nonlocal Bell measurement described above. Then, a Bell measurement with the same setup as shown by Fig. IV C on the two local ensembles 1 and 3, together with a straightforward displacement of X_3^a , P_3^a on the sample 3, will teleport an unknown collective spin state from the atomic ensemble 3 to 2. The teleported state on the ensemble 2 has the same form as that in the original proposal of continuous variable teleportation using squeezing light [67], with the squeezing parameter rreplaced by Eq. (27) and with an inherent Bell detection inefficiency $\eta = 1/(1+2\kappa_c^2)$. The quality of teleportation is best described by the fidelity, which, for a pure input state, is defined as the overlap of the teleported state and the input state. For any coherent input state of the sample 3, the teleportation fidelity is given by

$$F = 1 / \left(1 + \frac{1}{1 + 2\kappa_c^2} + \frac{1}{2\kappa_c^2} \right). \tag{28}$$

Equation (28) shows that a high fidelity $F \approx 96\%$ would be possible for the teleportation of the collective atomic spin state with the interaction parameter $\kappa_c \approx 5$.

In the experimental demonstration [44], the atomic ensembles are provided by room-temperature Cesium atomic gas in two separate glass cells with coated wall to increase the spin relaxation time. Each cell is about 3 cm long, containing about 10^{12} atoms. The entanglement is generated through collective Bell measurements by transmitting a coherent light pulse as described above. To confirm and measure the generated entanglement, one needs to transmit another verifying Trough a homodyne detection of this verifying pulse, one can basically detect the EPR variation $\Delta_{EPR} = \left[\delta \left(X_1^a - X_2^a \right)^2 + \delta \left(P_1^a + P_2^a \right)^2 \right] / 2$ [66], and $\xi = 1 - \Delta_{EPR}$ serves as a measure of the entanglement, which is zero for separable states and 1 for the maximally entangled state. In this experiment, ξ is measured to be (35 ± 7) %, and this entanglement survives by about 0.5 ms (the relaxation time is measured by changing the time delay between the entangling and the verifying pulses). The demonstrated entanglement will be important for the next-step applications.

V. CONCLUSIONS

During the last few years the fields of atomic physics and quantum optics have experienced an enormous progress in controlling and manipulating atoms with lasers. This has immediate implications for quantum information processing, since this progress allows atomic systems to fulfill the basic requirements to implement the basic building blocks of a quantum computer. In this article we have illustrated these statements with two particular systems: trapped ions, neutral atoms in optical lattices and atomic ensembles.

The physics of trapped ions is very well understood. In fact, with the recent experimental results we can foresee no fundamental obstacle to build a scalable quantum computer with trapped ions. Of course, technical development may impose severe restrictions to the time scale in which this is achieved. On the other hand, neutral atoms in optical lattices seem to be ideal candidates to study a variety of physical phenomena by using them to simulate other physical systems. This quantum simulation may turn out to be the first real application of quantum information processing. Atomic ensembles, on the other hand, are ideal to realize quantum communication protocols (e.g. the quantum repeater, and the entanglement of distant atomic ensembles) within setups which are considerably simpler from an experimental point of view than the single atom and ion experiments. There are other quantum optical systems that have experienced a very remarkable progress during the last years, and which may equally important in the context of quantum information. An example is cavity QED, where groups

at Caltech, Georgia Tech, Innsbruck, and Munich have trapped single atoms and ions inside cavities, and let them interact with the cavity field, which can be used as single (or entangled) photon(s) generators as well as to build quantum repeaters for quantum communication.

- M. Nielsen and I. Chuang. Quantum Computation and Quantum Information. Cambridge University Press, 2000.
- [2] S. Braunstein and A. K. Pati, editors. Quantum Information with Continuous Variables. Kluwer Academic Publishers, 2003.
- [3] J.I. Cirac, L.M. Duan, D. Jaksch, and P. Zoller. Quantum optical implementation of quantum information processing. In F. De Martini and C. Monroe, editors, Proceedings of the International School of Physics "Enrico Fermi" Course CXLVIII, Experimental Quantum Computation and Information. IOS Press, Amsterdam, 2002.
- [4] B. G. Levi. Physics Today, May 2003.
- [5] J. I. Cirac and P. Zoller. Science, 301:176, 2003.
- [6] J. M. Raimond, M. Brune, and S. Haroche. Rev. Mod. Phys., 73:565, 2001.
- [7] M. D. Lukin. 2003.
- [8] J. I. Cirac and P. Zoller. Phys. Rev. Lett., 74(20):4091, 1995.
- [9] A. Steane. Appl. Phys. B, 64:623, 1997.
- [10] F. Schmidt-Kaler, H. Häffner, M. Riebe, S. Gulde, G.P.T. Lancaster, T. Deuschle, C. Becher, C.F. Roos, J. Eschner, and R. Blatt. *Nature*, 422:408, 2003.
- [11] D. Leibfried, B. DeMarco, V. Meyer, D. Lucas, M. Barrett, J. Britton, W. M. Itano, B. Jelenkovi, C. Langer, T. Rosenband, and D. J. Wineland. *Nature*, 422:412, 2003.
- [12] D. Leibfried, B. DeMarco, V. Meyer, M. Rowe, A. Ben-Kish, M. Barrett, J. Britton, J. Hughes, W. M. Itano, B. M. Jelenkovic, C. Langer, D. Lucas, T. Rosenband, and D. J. Wineland. J. Phys. B, 36:599, 2003.
- [13] J. J. García-Ripoll, P. Zoller, and J. I. Cirac. Phys. Rev. Lett., 91:157901, 2003.
- [14] L.-M. Duan, J. I. Cirac, and P. Zoller. Science, 292:1695, 2001.
- [15] C. W. Gardiner and P. Zoller. Quantum Noise: A Handbook of Markovian and Non-Markovian Quantum Stochastic Methods with Applications to Quantum Optics. Springer, 1999.
- [16] D. J. Wineland, C. Monroe, W. M. Itano, D. Leibfried, B. E. King, and D. M. Meekhof. RES J. NIST, 103:259, 1998.
- [17] J. I. Cirac and P. Zoller. *Nature*, 404:579, 2000.
- [18] D. Kielpinksi, C. Monroe, and D. J. Wineland. *Nature*, 417:709, 2002.
- [19] A. Steane, C. F. Roos, D. Stevens, A. Mundt, D. Leibfried, F. Schmidt-Kaler, and R. Blatt. *Phys. Rev.* A, page 042305, 2000.
- [20] A. Sørensen and K. Mølmer. Phys. Rev. A, 62:022311, 2000.
- [21] A. Sørensen and K. Mølmer. Phys. Rev. Lett., 82(9):1971, 1999
- [22] D. Jonathan, M. B. Plenio, and P. L. Knight. Phys. Rev. A, 62:042307, 2000.
- [23] G. J. Milburn, S. Schneider, and D. F. V. James. Fortschritte der Physik, 48:801, 2000.

- [24] B. DeMarco, A. Ben-Kish, D. Leibfried, V. Meyer, M. Rowe, B. M. Jelenkovic, W. M. Itano, J. Britton, C. Langer, T. Rosenband, and D. J. Wineland. *Phys. Rev. Lett.*, 89:267901–1, 2002.
- [25] D. Jaksch, C. Bruder, J.I. Cirac, C. Gardiner, and P. Zoller. Phys. Rev. Lett., 81(15):3108, 1998.
- [26] D. Jaksch, H.J. Briegel, J.I. Cirac, C.W. Gardiner, and P. Zoller. Phys. Rev. Lett., 82:1975, 1999.
- [27] M. Greiner, O. Mandel, T. Esslinger, T.W. Hänsch, and I. Bloch. *Nature*, 415:39, 2002.
- [28] O. Mandel, M. Greiner, A. Widera, T. Rom, T.W. Hänsch, and I. Bloch. *Nature*, 425:937, 2003.
- [29] G. Brennen, C. Caves, P. Jessen, and I. Deutsch. *Phys. Rev. Lett.*, 82:1060, 1999.
- [30] G.K. Brennen, I.H. Deutsch, and C.J. Williams. *Phys. Rev. A*, 65:022313, 2002.
- [31] D. Jaksch, J. I. Cirac, P. Zoller, S.L. Rolston, R. Cote, and M. D. Lukin. *Phys. Rev. Lett.*, 85:2208, 2000.
- [32] S. Sachdev. Quantum Phase Transitions. Cambridge University Press, Cambridge, 1999.
- [33] T. Calarco, E.A. Hinds, D. Jaksch, J. Schmiedmayer, J.I. Cirac, and P.Zoller. Phys. Rev. A, 61:22304, 2000.
- [34] N. Schlosser, G. Reymond, I. Protsenko, and P. Grangier. Nature, 411:1024, 2001.
- [35] F.B.J. Buchkremer, R. Dumke, M. Volk, T. Muether, G. Birkl, and W. Ertmer. *Laser Physics*, 12:736, 2002.
- [36] R. Raussendorf and H. J. Briegel. *Phys. Rev. Lett.*, 86(22):5188, 2001.
- [37] E. Jane, G. Vidal, W. Dür, and P. Zoller. Quantum Information and Computation, 1:15, 2003.
- [38] S. Lloyd. Science, 273:1073, 1996.
- [39] M. D. Lukin, M. Fleischhuaer, R. Cote, L.-M. Duan, D. Jaksch, J. I. Cirac, and P. Zoller. *Phys. Rev. Lett.*, 87:037901, 2001.
- [40] L.-M. Duan, M. D. Lukin, J. I. Cirac, and P. Zoller. Nature, 414:413, 2001.
- [41] A. Kuzmich and E. S. Polzik. *Phys. Rev. Lett.*, 85(26):5639, 2000.
- [42] L.-M. Duan, J. I. Cirac, P. Zoller, and E. S. Polzik. Phys. Rev. Lett., 85(26):5643, 2000.
- [43] M. Fleischhauer and M. D. Lukin. Phys. Rev. Lett., 84(22):5094, 2000.
- [44] B. Julsgaard, A. Kozhekin, and E. S. Polzik. *Nature*, 413:400, 2001.
- [45] L.-M Duan. Phys. Rev. Lett., 88:170402, 2002.
- [46] A. Kuzmich, W. P. Bowen, A. D. Boozer, A. Boca, C. W. Chou, L.-M. Duan, and H. J. Kimble. *Nature*, 423:731, 2003
- [47] C. H. van der Wal, M. D. Eisaman, A. Andre, R. L. Walsworth, D. F. Phillips, A. S. Zibrov, and M. D. Lukin. Science, 301:196, 2003.
- [48] W. Jiang, C. Han, P. Xue, L. M. Duan, and G. C. Guo. quant-ph/0309175.
- [49] J. Hald, J. L. Sorensen, C. Schori, and E.S. Polzik. Phys. Rev. Lett., 83:1319, 1999.
- [50] L. V. Hau, S. E. Harris, Z. Dutton, and C. H. Behroozi.

- Nature, 397:594, 1999.
- [51] M. M. Kash, V. A. Sautenkov, A. S. Zibrov, L. Hollberg, G. R. Welch, M. D. Lukin, Y. Rostovtsev, E. S. Fry, and M.O. Scully. *Phys. Rev. Lett.*, 82:5229, 1999.
- [52] A. Kuzmich, L. Mandel, and N. P. Bigelow. Phys. Rev. Lett., 85(8):1594, 2000.
- [53] H. J. Briegel, W. Dur, J. I. Cirac, and P. Zoller. *Phys. Rev. Lett.*, 81(26):5932, 1998.
- [54] A. Ekert. Phys. Rev. Lett., 67(6):661, 1991.
- [55] C. H. Bennett, G. Brassard, C. Crepeau, R. Jozsa, A. Peres, and W. K. Woothers. *Phys. Rev. Lett.*, 70(13):1895, 1993.
- [56] C. H. Bennett, D. P. Divincenzo, J. A. Smolin, and W. K. Wootters. *Phys. Rev. A*, 54(5):3824, 1996.
- [57] J. Preskill. http://www.theory.caltech.edu/people/preskill/ph229/, Rev. Lett., 84:2722, 2000.
- [58] J. I. Cirac, P. Zoller, H. J. Kimble, and H. Mabuchi. Phys. Rev. Lett., 78(16):3221, 1997.
- [59] S.J. Van Enk, J.I. Cirac, and P. Zoller. Science, 279:205,

1998.

- [60] J. Ye, D. W. Vernooy, and H.J. Kimble. Phys. Rev. Lett., 83:4987, 1999.
- [61] A. Kuhn, M. Hennrich, and G. Rempe. Phys. Rev. Lett., 89:067901, 2002.
- [62] J. A. Sauer, K. M. Fortier, M. S. Chang, C. D. Hamley, and M. S. Chapman. quant-ph/0309052.
- [63] J. McKeever, A. Boca, A. D. Boozer, J. R. Buck, and H. J. Kimble. *Nature*, 425:268, 2003.
- [64] C. Cabrillo, J. I. Cirac, P. G-Fernandez, and P. Zoller. Phys. Rev. A, 59(2):1025, 1999.
- [65] L.-M. Duan, J.I. Cirac, and P. Zoller. Phys. Rev. A, 66:023818, 2002.
- [66] L.-M. Duan, G. Giedke, J. I. Cirac, and P. Zoller. *Phys.* 1200 (Page 1201).
- [67] S. L. Braunstein and H. J. Kimble. Phys. Rev. Lett., 80(4):869, 1998.